Complementary photothermal techniques for complete thermal characterization of porous and semi-transparent solids

D. Dadarlat · M. Streza · O. Onija ·
C. Prejmerean · L. Silaghi-Dumitrescu ·
N. Cobirzan · K. Strzałkowski

Abstract The paper is focused on the ability of using two complementary photothermal techniques for the measurement of all thermal parameters of some porous and/or semi-transparent solid samples whose composition, structure, and geometry do not allow a complete thermal characterization using a single technique. In this work, we combine a contact technique, photopyroelectric (PPE) calorimetry, with a non-contact one, infrared lock-in IR thermography (IRT), in order to investigate some solid samples such as dental composites, building materials, drugs, and semiconductors. The composition and the geometry of the investigated samples make the PPE method (in "front" detection configuration together with thermal-wave resonator cavity (TWRC) technique as scanning procedure) suitable for thermal effusivity measurements and IRT for thermal diffusivity investigations. In such a way, this combination of methods leads to a complete thermal characterization of the investigated materials.

Introduction

It is well known that the photopyroelectric (PPE) technique is now able to perform a complete characterization (measurement of static—volume-specific heat—and dynamic—thermal diffusivity, conductivity, and effusivity—thermal parameters) of a solid sample, if the requirements of the particular detection cases are fulfilled. In order to measure the dynamic thermal parameters mentioned before and to obtain particular detection cases of experimental interest, one has to perform some theoretical/experimental optimizations by acting especially on the number of layers and on the optical and thermal thickness of each layer of the detection cell. For the contact techniques such as PPE calorimetry, a perfect sensor/sample thermal contact is also crucial.

On the other hand, the solid materials under investigation present sometimes particularities acting against the requirements of the particular detection cases: they are transparent to the incident light or present rough surfaces; they can be obtained only as very thin layers (drugs) or opposite, only as bulk samples (building materials); the coupling fluid can penetrate inside the sample in the case of contact techniques, etc. Consequently, sometimes it is necessary to combine different techniques for a complete thermal characterization of the materials. Several attempts have been already successfully been reported; we cite here, as example, a contact (PPE)–non-contact (PTR) approach [1–3].

It is well known that the four thermal parameters, such as the static—volume-specific heat C, and the dynamic—thermal diffusivity α, conductivity k, and effusivity e, are

D. Dadarlat · M. Streza (✉) · O. Onija
National Institute for Research and Development of Isotopic and Molecular Technologies, 65-103 Donath Str, 400293 Cluj-Napoca, Romania
e-mail: streza.mihaela@gmail.com

C. Prejmerean · L. Silaghi-Dumitrescu
"Raluca Ripan" Institute for Research in Chemistry, 400294 Cluj-Napoca, Romania

N. Cobirzan
Department of Civil Engineering and Management, Faculty of Civil Engineering, Technical University of Cluj Napoca, 25 G. Baritiu Street, 400027 Cluj-Napoca, Romania

K. Strzałkowski
Institute of Physics, Faculty of Physics, Astronomy and Informatics, Nicolaus Copernicus University, Grudziadzka 5, 87-100 Torun, Poland

connected by two relationships, $k = C\alpha$ and $e = (Ck)^{1/2}$; in conclusion, only two are independent (the remaining two can be calculated). In such a way, this combination of methods leads to a complete thermal characterization of the materials. Usually, the photothermal methods allow the direct measurement of thermal diffusivity and effusivity; the remaining two thermal parameters can be then calculated [4, 5].

In this paper, we will combine a contact technique (PPE) with a non-contact one (IRT) in order to investigate some "special" samples as composite materials used in dentistry, drug industry and buildings, and some semiconductors. The composition and the geometry of the investigated samples make the PPE method (in "front" detection configuration together with thermal-wave resonator cavity (TWRC) technique as scanning procedure) suitable for thermal effusivity measurements and the lock-in thermography (IRT) for thermal diffusivity investigations [1–3].

Theoretical aspects

Front photopyroelectric configuration (FPPE)

In the PPE method, the temperature variation of a sample exposed to a modulated radiation is measured with a pyroelectric sensor, situated in intimate thermal contact with the sample [6, 7]. Concerning the PPE detection configurations, two of them, "back" and "front", respectively, have been mainly applied for calorimetric purposes. In this paper, we will use only the front one (FPPE), with the purpose of directly measuring the thermal effusivity of the investigated material. In the FPPE configuration, the radiation impinges on the front surface of the sensor, and the sample, in good thermal contact with its rear side, acts as a heat sink [8, 9]. We selected this configuration, because no special request is imposed on the sample's geometry; the solid under investigation (the backing layer) must be only thermally thick.

The layout of the FPPE detection configuration is classical: the cell contains three layers: a directly irradiated pyroelectric sensor of thickness L_p, a semi-infinite backing material (sample), and, between them, a coupling fluid with a variable thickness in the range L_l–L_p. The radiation is partially absorbed by the front, opaque electrode of a thermally thin pyroelectric sensor. Air and backing layers are considered as semi-infinite. The heat propagation through the layered system is considered as one-directional. In this approximation, the normalized complex FPPE signal is given by [10–13]:

$$V^{PPE} = \frac{[S(b_{bl}+1) - S^{-1}(b_{bl}-1)](\sigma_p L_p)}{(\sigma_p L_p)[S(b_{bl}+1) - S^{-1}(b_{bl}-1)] + b_{lp}[S(b_{bl}+1) + S^{-1}(b_{bl}-1)]}, \quad (1)$$

where

$$S = \exp(\sigma_l L_l), \quad \sigma_j = (1+i)a_j, \quad \mu = (2\alpha/\omega)^{1/2}, \quad b_{ij} = e_i/e_j. \quad (2)$$

In Eqs. (1–2), ω is the angular chopping frequency of radiation; σ and a are the complex thermal diffusion coefficient and the reciprocal of the thermal diffusion length, respectively. Symbols "p", "l", and "b", refer to pyroelectric sensor, liquid layer (acting as a coupling fluid in the PPE configuration), and backing material, respectively. The normalization of Eq. (1) was performed with the signal obtained with the sensor standing alone in air.

In order to compare results obtained with different coupling fluids and backing materials, it is useful to perform a second normalization with the signal obtained with very thick liquid layer. The result is given by

$$V_n^{PPE} = \frac{\sigma_p L_p + b_{lp}}{(\sigma_p L_p) + b_{lp}\left[\frac{1 - R_{bl}\exp(-2\sigma_l L_l)}{1 + R_{bl}\exp(-2\sigma_l L_l)}\right]}, \quad (3)$$

where

$$R_{ij} = (1 - b_{ij})/(b_{ij} + 1) \quad (4)$$

represents the reflection coefficient of the thermal wave at the "ij" interface.

Equation (3) indicates that the thermal effusivity of the backing material can be obtained by performing a coupling fluid's thickness scan of the phase of the FPPE signal, providing, however, a proper selection of the experimental parameters (chopping frequency, thickness scan range, thickness variation step) has been made.

Lock-in IR thermography

The principle of lock-in thermography is based on the application of a periodic input energy to the surface of the object and analyzing the thermal response of the investigated surface [14, 15]. A lock-in thermography system computes the modulated response of the local surface temperature recorded by an IR camera and outputs the resulted DC, amplitude, and phase images to a PC. The main advantage of lock-in thermography technique is that the signal-to-noise ratio can be improved by averaging the useful signal over many periods. This technique is a versatile tool for non-destructive evaluation (NDE). In this paper, we will use this technique for measuring the thermal diffusivity of the investigated materials. The idea is to calculate the thermal-wave phase shift when the heat diffuses into an isotropic and homogeneous medium with thermal diffusivity α. At a long distance from a punctual heat source, the thermal wave can be approximated as a plane wave, and it can be written as

$$T(x,t) = T_o e^{i(2\pi ft - \overrightarrow{k}\,\overrightarrow{x})}, \tag{5}$$

where $\overrightarrow{x}$ is the thermal-wave propagation direction, T_0 is the surface temperature, f is the excitation frequency, t is the time, and $\overrightarrow{k}$ is the wave vector. The thermal diffusion equation can be written as

$$\alpha \frac{\partial^2 T(x,t)}{\partial x^2} = \frac{\partial T(x,t)}{\partial t}. \tag{6}$$

For physical reasons, the solution of thermal wave must converge at infinity, which requires

$$\vec{k} = (1 - i)\sqrt{\frac{\pi f}{\alpha}}. \tag{7}$$

The thermal wave can be rewritten as follows:

$$T(x,t) = T_o e^{-\sqrt{\frac{\pi f}{\alpha}}x} e^{i\left(2\pi ft - \sqrt{\frac{\pi f}{\alpha}}x\right)}. \tag{8}$$

The propagation of a plane thermal wave through a medium of thickness x and thermal diffusivity α leads to a phase shift $\Delta\varphi$ having the following expression:

$$\Delta\varphi = -\sqrt{\frac{\pi f}{\alpha}}x = ax, \tag{9}$$

where a is the slope of the phase-distance graph. The thermal diffusion length is expressed by

$$\mu = \frac{1}{a} = \sqrt{\frac{\alpha}{\pi f}} \tag{10}$$

and can be deduced according to Eq. 9.

Experimental

Front photopyroelectric configuration

The experimental setup for FPPE experiments was extensively described elsewhere [2, 16]. The PPE sensor is a 15-mm diameter and 215-μm-thick LiTaO$_3$ sensor ($e_p = 3.6 \times 10^3$ W s$^{1/2}$ m^{-2} K^{-1}; and $\alpha_p = 1.1 \times 10^{-7}$ m^2 s^{-1}) coated with gold electrodes on both faces and glued onto a rotating stage. The backing material is situated on a micrometric stage. The modulated radiation (100 mW YAG laser) is partially absorbed by the front electrode of the sensor. The space between the sensor and the backing material accommodates the liquid layer. The liquid's thickness variation is performed with a step of 0.03 μm (9062M-XYZ-PPP Gothic-Arch-Bearing Picomotor), and the data acquisition was taken at the end of each 30-th step. The "rough" control of the liquid's thickness and the parallelism between backing and sensor are assured by 3 and 6–axis micrometric stages. During the scanning

procedure, the sample's thickness variation is very rigorously controlled, but the absolute sample's thickness is not precisely known. Its correct value is obtained as a result of a fitting procedure [16]. The coupling fluids were ethylene glycol ($e_1 = 890$ W s$^{1/2}$ m^{-2} K^{-1}; $\alpha_1 = 9.36 \times 10^{-8}$ m^2 s^{-1}) and water ($e_1 = 1{,}600$ W s$^{1/2}$ m^{-2} K^{-1}; $\alpha_1 = 14.42 \times 10^{-8}$ m^2 s^{-1}) with thickness ranging from 0 to 1 mm. In order to avoid the penetration of the coupling fluid in the porous samples, the surface of the samples was separated from the coupling fluid by a very thin (5-μm thick) laboratory film (parafilm "M"—Pechiney plastic packaging). The normalized signal is obtained with thermally thick (thickness larger than 700 μm) coupling fluid. All the measurements were performed at room temperature. The PPE signal was processed with a SR 830 lock-in amplifier.

Lock-in IR thermography

The IR setup included a heat source, a waveform generator, an infrared camera, and a computer for data acquisition. The intensity-modulated optical stimulation ($f_0 = 1$ Hz and 0.1 Hz) was delivered by an Nd:YAG laser (Laser-Quantum OPUS, with $\lambda = 532$ nm and $P_{max} = 0.5$ W). The IR camera (FLIR 7200 series, with a 256×320 pixel array of InSb detectors, sensitive in the 1.5–5.1 μm wavelength range, working at a sampling frequency of 100 Hz) recorded the changes in the surface temperature of the specimens (1px = 30 μm). The signals delivered by the infrared camera and the reference frequency f_0 were sent to the lock-in detection module incorporated into the camera, which output the continuous component image ($f = 0$) as well as the amplitude and phase images of the f-component to a PC. The optical axis of the camera was perpendicular to the investigated surface. The investigated materials have a circular shape with a diameter of about 15 mm and a thickness ranging from 1.5 to 10 mm. A thin layer (about 1 μm) of carbon was deposited on the surface of the samples in order to increase the emissivity.

Samples

II-VI binary semiconductors

The II-VI binary crystals were grown from the melt by the high-pressure high-temperature Bridgman method under Argon overpressure. As a starting material, high purity ZnTe and CdTe powders were used. The crystal rods were cut into plates of 10-mm diameter and 1.3-mm thick, and mechanically grounded and polished with diamond paste. For IRT measurements, the incident surface of the samples was blackened with a thin layer of carbon.

Building materials

Saving energy in residential buildings sectors becomes the most important objectives of the researchers, designers, and entire our society. An energy-efficient building can increase design and executions' costs up to 15 % as compared to buildings designed on traditional principles but can decrease by 85 % the heating, cooling, and lightening costs during exploitations, creating in the same time an eco-friendly and healthy building (free from toxic substances) with low impact on the environment during their lifecycle. An efficient building material from thermotechnical point of view has a low thermal conductivity and low embodied energy coefficients.

In Romania, volcanic tuffs (sample TUF) are spread out on wide areas from Transylvanian Basin to Apuseni intermountain areas and the Carpathian mountains. The XRd analysis on tuff sample shows the presence of clinoptilolite (~ 64 %), quartz (25 %) and phillipsite (11 %). Zeolitic tuffs are thermal efficient building materials, leading to heat thermal stability of the buildings, due to their property to absorb heat during day and releasing out (inside the room) during the night. Generally, tuffs have a low density (1.627 g cm^{-3}), a high porosity (~ 21 %) was resulted from high zeolite content (~ 70 %), a low thermal conductivity, a medium thermal diffusivity and effusivity, and low embodied energy (~ 0.6 MJ kg^{-1}).

In building material, industry volcanic tuff not only is used as a rock, due to low heat conductivity, compared to other traditional building materials (solid ceramic brick or concrete) but can also be used for preparation of mortars (as aggregates or cement substitutes) light concrete, or to produce thermal and acoustical insulation materials. Mortars based on zeolitic tuffs (sample 31C in our paper) contain tuff as aggregate substituent, cement as binder and water, while traditional mortar contains cement, sand, and water (sample C1 in the experiment).

Drugs

An antihistaminic drug, the promethazine hydrochloride (PTZ), was selected for investigations. A saturated solution of PTZ starting material in tetrahydrofyran was prepared at room temperature, where it was maintained for 3–4 h. After filtration, an anti-solvent (heptane) is slowly added until a white precipitated is obtained. Then, it was slurred in acetonitrile, at room temperature for at least 4 h. The obtained powder was pressed at 50 atm and prepared as a disk of 8-mm diameter and 4-mm thick.

Dental-filling materials (giomers)

Giomers represent a new concept in restorative dentistry, based on novel pre-reacted glass technology, where special glass-ionomer fillers are included in the resin matrix. The resin matrix of the giomers comprises aromatic dimethacrylates/urethane dimethacrylates as base monomers and aliphatic methacrylates as diluting monomers. An adhesive system is used in combination with giomers in order to obtain a dental restoration. Commercial Beautifil II giomer was used in our experiments after solidification as a cylindrical sample of 8-mm diameter and 10-mm thick.

It is well known that, in principle, the PPE calorimetry is able to directly measure both thermal effusivity and diffusivity of a solid sample, by combining the two back and front configuration, if the sample can be processed with a given geometry: thin opaque disks in the BPPE configuration and thick (one flat surface) materials in the FPPE [16].

For the materials mentioned before, the request of the BPPE configuration cannot be fulfilled, because they are porous (TUF), transparent to incident radiation when processed as thin layers (giodent, semiconductors), or they are pressed powders that are not mechanically resistant as thin layers (PTZ). In such cases, a different non-contact method (IRT for example) must be used.

Results

In the following, the results, obtained on the investigated materials by using the contact and non-contact technologies, are presented.
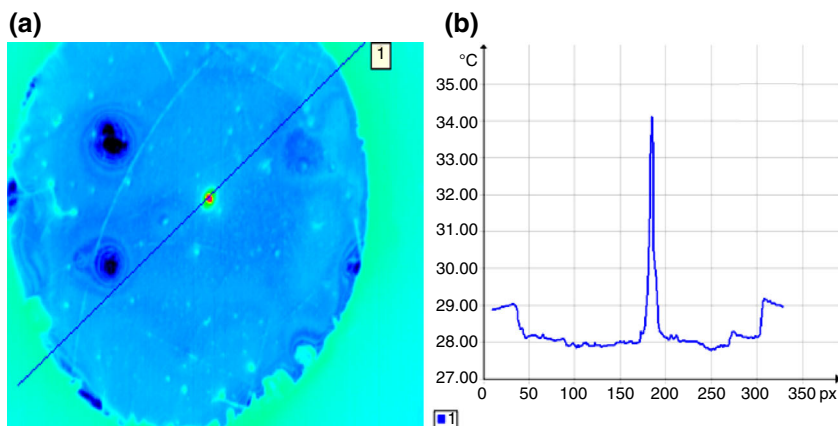
II-VI binary semiconductors

Figure 1 displays the normalized phase of the FPPE signal, as a function of the coupling fluid's thickness for the investigated CdTe and ZnTe binary semiconductors, together with the values obtained for the thermal effusivity. The results obtained on the same materials by using IRT are displayed in Figs. 2–5. Figure 2a shows the DC image for CdSe, and Fig. 2b represents the profile of this image along the marked line. Because the emissivity coefficient of the surface varies sharply in the presence of surface roughness, the DC image is typically disturbed, and the image is very noisy. Using the lock-in detection system, the images of the magnitude and phase at the excitation frequency f have been obtained (see Figs. 3a, 4a). These images are mostly free of artifacts induced by surface roughness, and they feature a higher contrast. Figures 3b and 4b show the corresponding profiles along the indicated lines. From Fig. 4b, one can identify the laser impact area (represented by the constant phase zone), and we can evaluate the extent of the heat diffusion region around the excitation zone (120px, 1px = 30μm). The phase profiles

for ZnTe and CdTe are shown in Fig. 5a, b. The average values of thermal diffusivities were calculated according to Eq. (9).
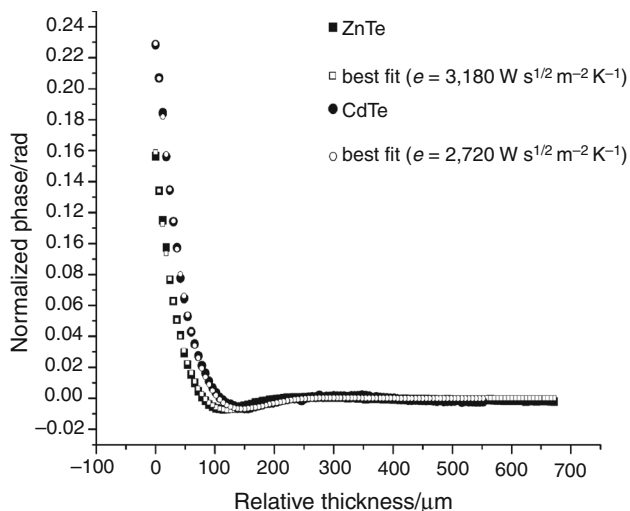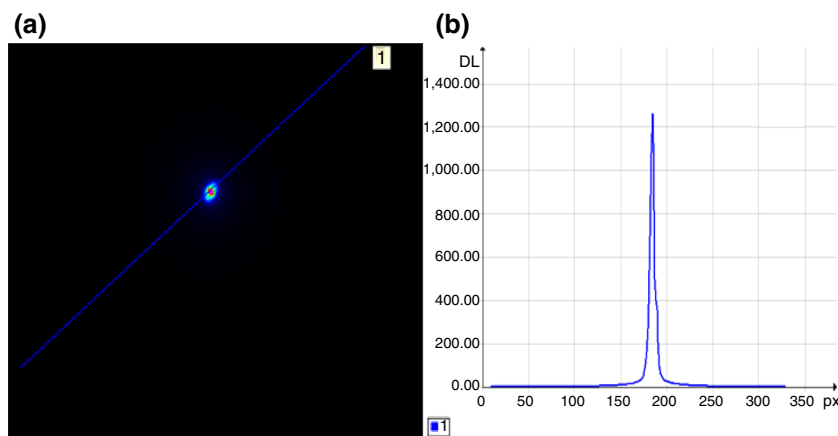

Fig. 1 Normalized phase of the FPPE signal, as a function of the coupling fluid's thickness for II-VI binary semiconductors. Ethylene glycol was used as coupling fluid, and the chopping frequency was 3 Hz. The best fit for each sample is also displayed (*empty symbols*)
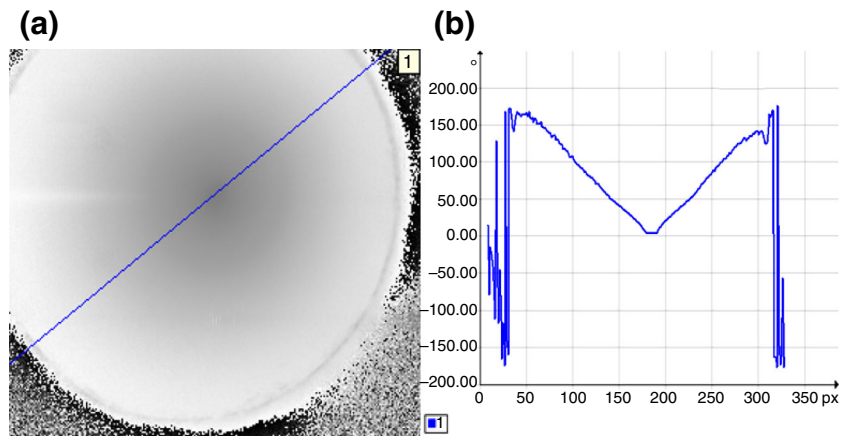
Building materials

Typical results for the normalized phase of the FPPE signal, as a function of the coupling fluid's thickness, obtained for the investigated building materials are displayed in Fig. 6. Figure 7 reveals the phase image for a mortar based on zeolitic tuff (31C) at 0.2 Hz excitation frequency, and Fig. 8 shows the corresponding phase profile. Similar investigations were performed for a classical mortar and volcanic tuff. This type of mortar (31C) has a lower thermal conductivity coefficient and an increased thermal effusivity compared to classical mortar (see Table 1).

Drugs (PTZ) and dental-filling materials (giomers)

Typical results for the normalized phase of the FPPE signal, as a function of the coupling fluid's thickness, obtained for PTZ and Beautifil II giomer are displayed in Fig. 9. The IRT experiments were performed as described before, and the results obtained for the values of thermal diffusivity were $\alpha = 2.4 \cdot 10^{-7} \, m^2 \, s^{-1}$ for PTZ, and $\alpha = 0.8 \cdot 10^{-7} \, m^2 \, s^{-1}$ for giomer.

Table 1 contains a synthesis of the results obtained on all the investigated materials, together with the calculated

Fig. 2 The continuous (DC) image (**a**) and the profile of the image (**b**) along the marked line for ZnTe at 1 Hz excitation frequency

Fig. 3 The amplitude image (**a**) and the corresponding profile (**b**) along the marked line for ZnTe at 1 Hz excitation frequency

Fig. 4 The phase image (**a**) and the corresponding profile (**b**) along the marked line for ZnTe at 1 Hz excitation frequency

Fig. 5 The phase profiles as a function of distance traversed by heat wave for ZnTe (**a**) and CdTe (**b**) at 1 Hz excitation frequency
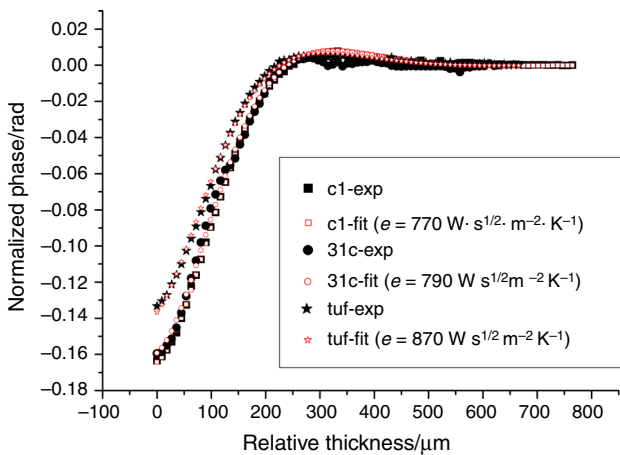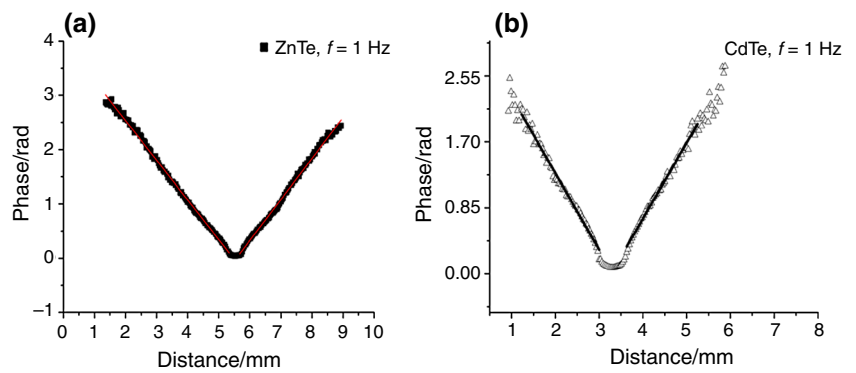
Fig. 6 Normalized phase of the FPPE signal, as a function of the coupling fluid's thickness for investigated building materials. Water was used as coupling fluid, and the chopping frequency f = 1 Hz. The best fit for each sample is also displayed (*empty symbols*)

values for the thermal conductivity and the data reported in the literature.

Concerning semiconductors, some inconsistencies between the thermal conductivity of the investigated crystals obtained in this study and the literature data

were found. In our opinion, this is mainly due to the fabrication process of the crystals and to the quality of their structure.

Concerning building materials, the thermal diffusivity and effusivity are sensitive parameters determining their use as thermal isolators. The thermal effusivity is a measure of a materials ability to exchange thermal energy with its surroundings, while the thermal diffusivity of a material is a measure of how fast the material temperature adapts to the surrounding temperature. The thermal diffusivity of a building material influences the penetration dept and speed of temperature adaption under a varying thermal environment, but it says nothing about the energy flows. On the other hand, the thermal effusivity influences the ability to exchange thermal energy with its surroundings. In building materials with a high thermal effusivity, high-temperature differences are associated with a high energy flux. The building materials investigated in this paper have similar thermal conductivity (0.47–0.97 Wm^{-1} K^{-1}) and effusivity (770–870 $Ws^{1/2}$ m^{-2} K^{-1}). These thermal parameters are very close to those of asphalt and gypsum. Concerning the thermal diffusivity, it is higher in the case of C1

Fig. 7 The phase image (**a**) and the corresponding profile (**b**) along the marked line for 31C tuff at 0.2 Hz excitation frequency
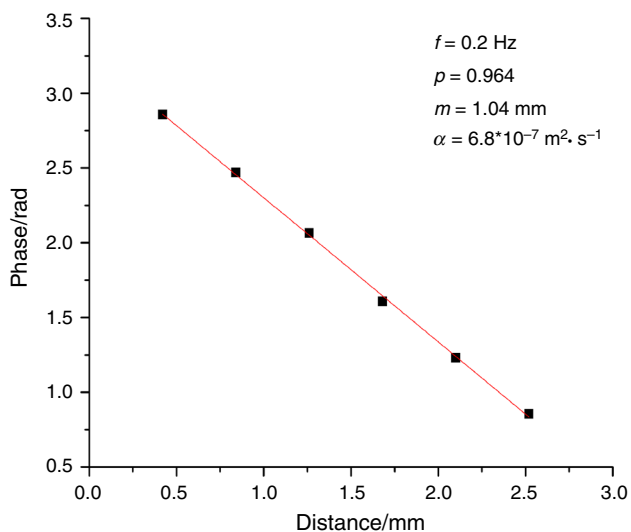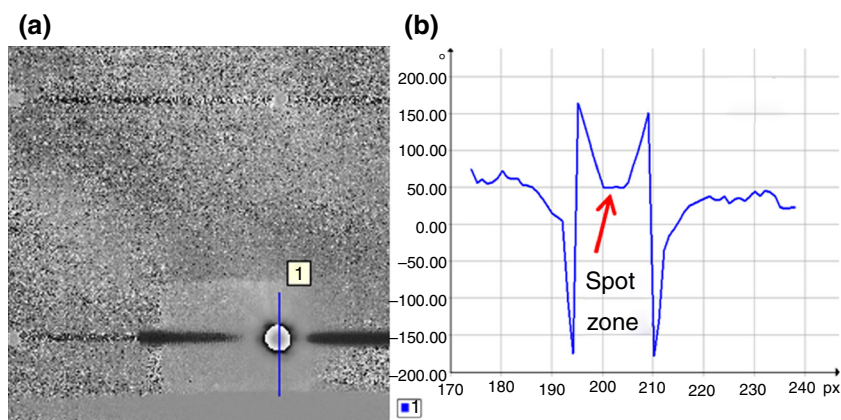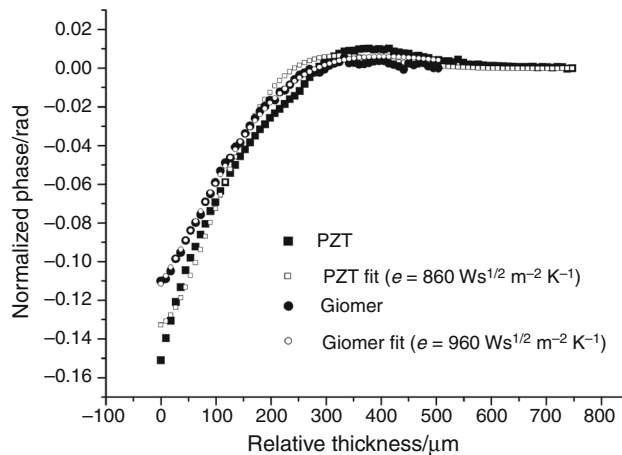

Fig. 8 The phase profiles as a function of distance traversed by heat wave for 31C tuff at 0.2 Hz excitation frequency

Fig. 9 Normalized phase of the FPPE signal, as a function of the coupling fluid's thickness for giodent and for PTZ. Water was used as coupling fluid, and the chopping frequency was 1 Hz for PTZ and 0.5 Hz for Beautifil II giomer. The best fit for each sample is also displayed (*empty symbols*)

Table 1 Room temperature values of the thermal parameters of the investigated materials

Material	Thermal effusivity/ W s$^{1/2}$ m^{-2} K^{-1}	10^7 Thermal diffusivity/ m^2 s^{-1}	Thermal conductivity/ W m^{-1} K^{-1}
CdTe	2,720	31.3	4.81 (7.1 [20])
ZnTe	3,180	55.0	7.46 (18.0 [20])
C1	770	16.0	0.97
31C	790	6.8	0.65
TUF	870	3.0	0.47
PTZ	860	2.4	0.42
Beautifil II	960	0.8	0.27

compared with 31C and TUF, but all of them are lower than in the case of other building materials as rockwool and/or sandstone.

The investigated drug material (PTZ) is in fact a disk-contained pressed powder. Consequently, the obtained thermal properties characterize the pill and not the material contained in the tablet. In order to find the properties of (or close to) the material, high pressures must be used when preparing the sample.

The thermal parameters obtained for the dental filler (Beautifil II giomer) indicate a good thermal biocompatibility of the material with the tooth.

Conclusions

The paper describes two contact and non-contact methods [(PPE) and lock-in thermography] for thermal characterization (measurement of thermal diffusivity, thermal effusivity, and thermal conductivity, respectively) of some solid samples which are difficult to be measured by other

methods, due to their structure. The composite materials selected for these investigations are porous samples (TUF), dental materials (giodent), and semiconductors (which are transparent when processed as thin layers), or they are pressed powders that are not mechanically resistant as thin layers (PTZ). Due to their "special" properties, these materials cannot be completely characterized using only one type of calorimetry (PPE for example), and this is why a coupled contact-non-contact methodology was necessary.

It was demonstrated that, for such type of materials, the PPE method (in "front" detection configuration, together with the TWRC technique as scanning procedure) is suitable for thermal effusivity measurements and the IRT for thermal diffusivity investigations. The remaining two thermal parameters (thermal conductivity and volume-specific heat) can be then calculated.

By combining the two methods, we tried, not only to avoid the geometrical/compositional problems caused by the samples, but also to increase the accuracy of the investigations. For example, in the FPPE configuration, the TWRC technique allows for a complete control (type and thickness variation) of the coupling fluid; the type of coupling fluid was selected to have an effusivity as close as possible to the samples, in order to increase the accuracy of the results [17]. The IRT technique, used for thermal diffusivity investigations, eliminates the problems connected with the presence of a coupling fluid (with unknown thickness–PPE) between the sample and sensor [18]. In building material industry, for example (which deals with porous materials), the thermal conductivity is crucial for thermal transfer computations, and the measurement of this parameter is time consuming. The accuracy in measurement is generally poor, being performed by a classical steady-state method [19]: a sample of unknown conductivity is placed between two brass plates with the hot brass plate at the top and the cold brass plate at the bottom. Heat is supplied at the top and made to move downward to stop any convection within the sample. Measurements are taken after the sample has reached to the steady state (with zero heat gradient or constant heat over entire sample), usually taking about 30 min and over, whereas a lock-in experiment is very fast, taking several tens of seconds. Even more, the IRT is suitable for the investigation of large areas, allowing for investigations in various points, being able to provide a 2D diffusivity map of samples having complex structures.

References

1. Dadarlat D, Pop MN, Streza M, Longuemart S, Depriester M, Sahraoui AH, Simon V. Combined FPPE–PTR calorimetry involving TWRC technique. Theory and mathematical simulations. Int J Thermophys. 2010;31:2275–82.
2. Dadarlat D, Pop MN, Streza M, Longuemart S, Depriester M, Sahraoui AH, Simon V. Combined FPPE-PTR calorimetry involving TWRC technique II. Experimental: application to thermal effusivity measurements of solids. Int J Thermophys. 2011;32:2092–101.
3. Dadarlat D. Contact and non-contact photothermal calorimetry for investigation of condensed matter. Trends and recent developments. J Therm Analysis Calor. 2012;110:27–35.
4. Dadarlat D, Pop MN, Onija O, Streza M, Pop MM, Longuemart S, Depriester M, Sahraoui AH, Simon V. Photopyroelectric (PPE) calorimetry of composite materials. J Therm Analysis Calor. 2013;111:1129–32.
5. Silaghi-Dumitrescu L, Dadarlat D, Streza M, Buruiana T, Prodan D, Hodisan I, Prejmerean C. Preparation of a new type of giomers and their thermal characterization by photopyroelectric calorimetry. Comparison with commercially available materials. J Therm Analysis Calor. 2014;. doi:10.1007/s10973-013-3561-x.
6. Mandelis A, Zver MM. Theory of the photopyroelectric effect in solids. J Appl Phys. 1985;57:4421–30.
7. Chirtoc M, Mihailescu G. Theory of the photopyroelectric method for investigation of optical and thermal materials properties. Phys Rev. 1989;B40:9606–17.
8. Dadarlat D, Chirtoc M, Neamtu C, Candea R, Bicanic D. Inverse photopyroelectric detection method. Phys Stat Sol. 1990;121:K231–4.
9. Dadarlat D, Frandas A. Inverse photopyroelectric detection of phase transitions. Appl Phys. 1993;A56:235–9.
10. Mandelis A, Matvienko A. Pyroelectric Materials and Sensors. 2007 (Kerala: D. Remiens): 61.
11. Delenclos S, Chirtoc M, Sahraoui AH, Kolinsky C, Buisine JM. Assessment of calibration procedures for accurate determination of thermal parameters of liquids and their temperature dependence using the photopyroelectric method. Rev Sci Instrum. 2002;73:2773–80.
12. Shen J, Mandelis A. Thermal-wave resonator cavity. Rev Sci Instrum. 1995;66:4999–5005.
13. Shen J, Mandelis A, Tsai H. Signal generation mechanism, intercavity-gas thermal diffusivity temperature dependence and absolute infrared emissivity measurements in a thermal-wave-resonant cavity. Rev Sci Instrum. 1998;69:197–203.
14. Busse G, Wu D, Karpen W. Thermal wave imaging with phase sensitive modulated thermography. J Appl Phys. 1992;71:3962–5.
15. Breiteinstein O, Warta W, Langenkamp M. Lock-in thermography: basics and use for evaluating electronic devices and materials. Berlin: Springer. 2012, ISBN: 3642024165.
16. Streza M, Pop MN, Kovacs K, Simon V, Longuemart S, Dadarlat D. Thermal effusivity investigations of solid materials by using the thermal-wave-resonator-cavity (TWRC) configuration. Theory and mathematical simulations. Laser Phys. 2009;19:1340–4.
17. Dadarlat D. Photopyroelectric calorimetry of liquids. Recent development and applications. Laser Phys. 2009;19:1330–9.
18. Salazar A, Oleaga A. Overcoming the influence of the coupling fluid in photopyroelectric measurements of solid samples. Rev Sci Instrum. 2012;83:014903.
19. Reiter M, Hartman H. A new steady-state method for determining thermal conductivity. J Geophys Res. 2012;76:7047–51.
20. Madelung O. Semiconductors: data handbook. Springer-Verlag; 2003.